FREQUENCY-DOMAIN AND TIME-DOMAIN RESPONSE SHAPING FOR ULTRA-WIDE BAND ANTENNAS

Razvan D. TAMAS[1]

Rezumat. *Această lucrare prezintă o metodă de sinteză pentru antene de bandă ultra-largă (UWB), având la bază profile cu pantă variabilă. Aplicând metoda în domeniul timp, este posibilă sintetizarea unor structuri radiante utilizabile în regim de impuls, concepute astfel încât să radieze un impuls cu distorsiuni reduse într-o anumită direcție și pentru o anumită polarizare.Metoda a fost validată prin sintetizarea unor antene de bandă ultra-largă special concepute pentru o anmită formă de undă a excitației. Aplicabilitatea metodei în domeniul frecvență a fost demonstrată sintetizând o antenă cu o variație cvasiliniară a câștigului într-o anumită gamă de frecvență. În vederea validării metodei, configurația rezultată din sinteză a fost simulată, fabricată și măsurată.*

Abstract. *This paper presents a synthesis approach for ultra-wide band (UWB) antennas, based on a variable slope profile. When applying the proposed approach in the time-domain, one can synthesize antenna structures for pulsed excitation, designed to yield a low distortion response at a given direction or within a given plane and for a given polarization. The method is validated by synthesizing ultra-wide band antennas designed for a particular waveform of excitation. The applicability of our method to frequency-domain synthesis is demonstrated by designing an antenna with a quasi-linear gain variation over a given frequency range. The antenna configuration resulting from synthesis was simulated, manufactured and measured in order to validate our method.*

Keywords: Ultra-wide band antennas, frequency-domain response shaping, time-domain response shaping, variable slope profile

DOI [10.56082/annalsarsciinfo.2024.2.5](https://doi.org/10.56082/annalsarsciinfo.2024.2.5)

1. Introduction

Due to the increasing interest in Ultra-Wide Band (UWB) communications, novel approaches have been developed and new descriptors have been defined [1, 2], [3-5], in order to analyze and evaluate the behavior of antennas with pulsed excitations.

[1]Title: Prof. Dr-Habil, affiliation: Department of Electronics and Telecommunications, Constanta Maritime University, Constanta, Romania, associate member of the Academy of Romanian Scientists (e-mail: tamas@ieee.org).

There are mainly two ways to conceive an UWB antenna: either by modeling and optimizing a given antenna design [6-8], or by synthesis. The synthesis may be oriented either towards continuous sources, or towards arrays [9-13], and may be performed either in the frequency-domain, or in the time-domain.

Synthesis of continuous sources is obviously more complicated, but technologically preferred. Some approaches are based on an initial design which is iteratively optimized by using specific algorithms, in terms of classical descriptors such as directivity [14] or bandwidth [15], or in terms of novel descriptors, such as overall fidelity [16] or similarity of the time-domain, electric field waveforms radiated at different directions [17].

Most of the usual UWB antennas [18] are not designed for a specific activation waveform. The overall fidelity of a communication system is generally improved through equalization techniques, by using different antennas for transmitting and receiving [19].

Some applications (e.g., military) require pulse-matched antennas with a relatively small width-to-height ratio. For such a low profile antenna, the main challenge would be to provide a good fidelity figure for a specific pulsed waveform along with an acceptable return loss at the input.

In this paper, we present a variable slope profile synthesis approach.

When applying our approach in the time-domain, one can synthesize antennas with a pulse-matched response. The goal of the synthesis is to design antennas with a low distortion (fidelity factor close to one) at a desired direction or within a plane, for a given polarization, and for a given activating waveform. The method is based on an approximate, finite expansion of the time-domain, far-field response of the antenna. The terms in the finite expansion are time-domain responses of short wire segments, each of them with a given slope with respect to the desired direction of polarization. The weights in that expansion; i.e., the cosines of the current angle of the profile with respect to the direction of polarization are computed by using a method of moments (MoM) type technique, in order to synthesize the physical design. Such pulse-matched antennas are finally synthesized, simulated and measured. One of them is a low-profile, spiral dipole which is able to provide a good fidelity factor within a plane perpendicular to its core.

A frequency-domain approach [21] might be preferred when a given response is needed over a frequency range. As an example, antennas with a flat or quasi-flat response over a given frequency range are commonly used in measuring systems or spark detection and localization systems. By implementing the resulting shape as a patch antenna [22] one can achieve a good input matching for a large variety of profiles. The frequency-domain approach was eventually validated for an

antenna with a quasi-flat response which was also fabricated and measured by using a method that we have previously developed [23].

The paper is organized as follows. In Section II the theoretical basis of our approach is presented, both in the frequency-domain and in the time-domain. Section III presents an example of frequency-domain response shaping, and Section IV, an example of time-domain response shaping. Conclusions are drawn in Section V.

2. Theory

The far-field produced by an antenna can be approximated to some extent by a finite expansion of time-domain responses of short, straight current filaments. Given a direction of polarization, the far-field contribution of each current filament can be weighted by properly choosing its slope. That finite expansion can be derived by sampling the integral expression of the electric field.

We firstly consider a straight, symmetrical dipole of a total length of 2*l* (Figure 1), driven by an arbitrary voltage waveform, $v_g(t)$. The frequency-domain, far electric field radiated at a perpendicular direction can be written as

$$\widetilde{E}_\theta(\theta=\pi/2,\omega)=\frac{\eta_0}{4\pi c_0 r}\int_{-l}^{l} j\omega I(z',\omega)\cdot\exp\left(-j\omega\frac{r}{c_0}\right)\mathrm{d}z'=\frac{\eta_0}{2\pi c_0 r}\int_{0}^{l} j\omega I(z',\omega)\cdot\exp\left(-j\omega\frac{r}{c_0}\right)\mathrm{d}z', \quad (1)$$

where η_0 is the free space wave impedance, c_0 is the speed of light, and $I(z',\omega)$ is the frequency-domain current distribution. Prime notations refer to source points on the antenna.

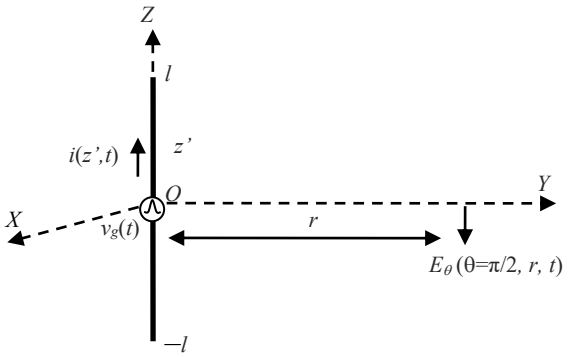

Fig. 1. Radiation from a dipole

We can assimilate the dipole to a degenerated, open-ended transmission line. Consequently,

$$I(z',\omega)=\frac{V_g(\omega)}{2Z_c}\left[\exp\left(-j\omega\frac{z'}{c_0}\right)-\exp\left(-j\omega\frac{2l-z'}{c_0}\right)\right] \tag{2}$$

where $V_g(\omega)$ is the Fourier transform of $v_g(t)$.

A frequency-domain, normalized electric field, $\widetilde{e}_t$ can be defined by compensating the effects of the propagation; i.e., attenuation and time delay,

$$\widetilde{e}_t(\theta=\pi/2,\omega)=r\cdot\widetilde{E}_\theta(\theta=\pi/2,\omega)\cdot\exp\left(j\omega\frac{r}{c_0}\right)=\frac{j\omega\eta_0 V_g(\omega)}{4\pi c_0 Z_c}\int_0^l\left[\exp\left(-j\omega\frac{z'}{c_0}\right)-\exp\left(-j\omega\frac{2l-z'}{c_0}\right)\right]\mathrm{d}z'. \tag{3}$$

Now, we consider a planar, curvilinear dipole (Figure 2) supposed to yield a non-distorted field at a specific direction, e.g. the perpendicular one; let γ' be the curvilinear coordinate along its symmetrical arms and $i(\gamma', t)$ the time-domain current distribution. The shape of the dipole arms is still to be found. This is a common problem to be solved in practice and planar antennas are often technologically convenient.

Referring to Figure 2, the contribution to E_θ of each elementary radiator on the contour is weighted by properly choosing the local slope of the profile i.e., the cosine of the current angle with respect to the *OZ* axis,

$$\varepsilon(\gamma')=\cos\theta'(\gamma')=\frac{\dfrac{\mathrm{d}z'}{\mathrm{d}x'}}{\sqrt{1+\left(\dfrac{\mathrm{d}z'}{\mathrm{d}x'}\right)^2}}. \tag{4}$$

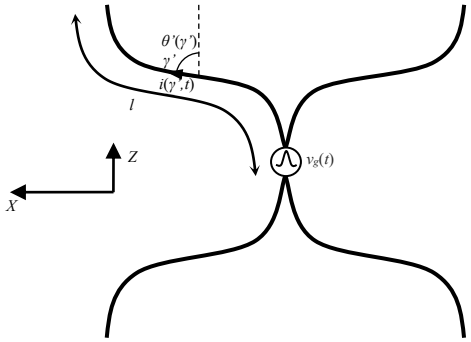

Fig. 2. Curvilinear wire dipole

Thus, a normalized electric field defined as in (3) can be found,

$$\widetilde{e}_t(\theta=\pi/2,\varphi=\pi/2,\omega)=\frac{j\omega\eta_0 V_g(\omega)}{4\pi c_0 Z_c}\left[\int_0^l\varepsilon(\gamma')\exp\left(-j\omega\frac{\gamma'}{c_0}\right)\mathrm{d}\gamma'-\int_0^l\varepsilon(\gamma')\exp\left(-j\omega\frac{2l-\gamma'}{c_0}\right)\mathrm{d}\gamma'\right]. \tag{5}$$

By substituting γ' with $2l-\gamma'$ in the last integral in (5) we have

$$\tilde{e}_t(\theta=\pi/2,\varphi=\pi/2,\omega)=\frac{j\omega\eta_0 V_g(\omega)}{4\pi c_0 Z_c}\left[\int_0^l \varepsilon(\gamma')\exp\left(-j\omega\frac{\gamma'}{c_0}\right)\mathrm{d}\gamma'-\int_l^{2l}\varepsilon(2l-\gamma')\exp\left(-j\omega\frac{\gamma'}{c_0}\right)\mathrm{d}\gamma'\right]. \tag{6}$$

By defining

$$e(\gamma')=\begin{cases}\varepsilon(\gamma'), \text{ for } 0\le\gamma'\le l,\\ -\varepsilon(2l-\gamma'), \text{ for } l<\gamma'\le 2l,\end{cases} \tag{7}$$

it is found that

$$\tilde{e}_t(\theta=\pi/2,\varphi=\pi/2,\omega)=\frac{j\omega\eta_0 V_g(\omega)}{4\pi c_0 Z_c}\int_0^{2l} e(\gamma')\exp\left(-j\omega\frac{\gamma'}{c_0}\right)\mathrm{d}\gamma'. \tag{8}$$

As expected, in order to design an antenna with a given frequency-domain response, the profile function $e(\gamma')$ can be found by performing an inverse Fourier transform on the transfer function. Finite support constraints actually would lead to an approximation of the desired frequency-domain response.

In the time-domain, it comes out from (8) that the profile of an antenna radiating a non-distorted waveform at that direction can be found by solving an integral equation; that is,

$$\int_0^{2l} e(\gamma')\frac{\mathrm{d}}{\mathrm{d}t}v_g\left(t-\frac{\gamma'}{c_0}\right)\mathrm{d}\gamma'=k\cdot v_g(t) \tag{9}$$

in which k is a constant and $e(\gamma')$ is the profile function to be found. The integral equation can actually be solved in a discrete form by applying a method of moments (MoM) type approach.

A discrete form of (9) can be derived by approximating

$$e(\gamma')\approx\sum_{n=1}^{N} e_n\delta(\gamma'-\gamma_n'). \tag{10}$$

We take as an excitation $v_g(t)$ a pulse of a finite time support, t_{supp}. The pulse travels from the voltage source towards the open end of the antenna and back to the source within a time slice of $2l/c_0$. For a good radiation efficiency, we assume that $t_{\mathrm{supp}}<2l/c_0$. In order to cover the whole time slice with full-support, delayed versions of $\mathrm{d}v_g/\mathrm{d}t$, one can take

$$\gamma_n'=(n-1)\frac{2l/c_0-t_{\mathrm{supp}}}{N-1}. \tag{11}$$

Consequently, the following finite expansion can be derived from (9),

$$\sum_{n=1}^{N} e_n\cdot\frac{\mathrm{d}}{\mathrm{d}t}v_g\left[t-(n-1)\frac{2l/c_0-t_{\mathrm{supp}}}{N-1}\right]=k\cdot v_g(t)+err(t) \tag{12}$$

in which *err*(*t*) gives the deviation from the excitation waveform.

It is clear from (8) that the expansion in (12) should contain pairs of weights of equal magnitude and opposite sign, since part of the radiation is due to the current reflected at the open end of the antenna. That can be easily accomplished for v_g odd or even since its derivative would be of opposite parity. In practice, most of the excitations are either odd, or even. For *N* odd, one can choose $e_{(N+1)/2}=0$, since $e_{(N-1)/2}=-e_{(N+3)/2}$.

Further, the coefficients e_n can then be computed by taking in (12) $t=m\Delta t$ with $m=\overline{1,N}$. By assuming *err*(*t*)=0, a matrix form of (12) can be derived,

$$\mathbf{G}\cdot\mathbf{E}=\mathbf{V} \tag{13}$$

where $\mathbf{E}=[e_1\ e_2\ \ldots\ e_N]^T$, $\mathbf{V}=[v_g(\Delta t),\ v_g(2\Delta t)\ \ldots\ v_g(N\Delta t)]^T$, and **G** is a *N*-by-*N* matrix with $G_{m,n}=\frac{\mathrm{d}}{\mathrm{d}t}v_g\left[m\Delta t-(n-1)\frac{2l/c_0-t_{\mathrm{supp}}}{N-1}\right]$.

Finally, it is found that

$$\mathbf{E}=\mathbf{G}^{-1}\cdot\mathbf{V}\,. \tag{14}$$

It should be noted that by solving equation (13) a continuous, piecewise-straight wire profile is obtained, with e_n the cosine of the angle between the *n*-th segment and the *OZ* axis.

An obvious interpretation can be given to the Fourier transform of (12),

$$V_g(\omega)\left\{\frac{k}{j\omega}-\sum_{n=1}^{N}e_n\cdot\exp\left[-j(n-1)\omega\frac{2l/c_0-t_{\mathrm{supp}}}{N-1}\right]\right\}=ERR(\omega). \tag{15}$$

A continuous, integral representation of (15) on an infinite length support would lead to a zero-error term if the current projection on the *OZ* axis is constant. That is, the antenna should be either an infinitely long, straight dipole or an infinitely long bowtie antenna. Such ideal antennas are known as being of an infinite bandwidth.

3. Frequency-domain response shaping

Antennas with a flat or quasi-flat response over a given frequency range (Figure 3) are commonly used in measuring systems or in spark detection and localization systems.

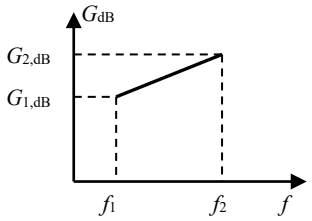

Fig. 3. Linear gain variation over a frequency range

The antennas to be synthesized are patch dipoles (Figure 4), as these antennas generally provide a good input matching for a myriad of shapes. It can be assumed that for such a patch dipole antenna, the current distribution is mainly focused on the contour of the radiating elements. Moreover, the current variations along the contour with respect to the curvilinear coordinate γ' can be assumed to be sinusoidal, as for an open ended transmission line [24].

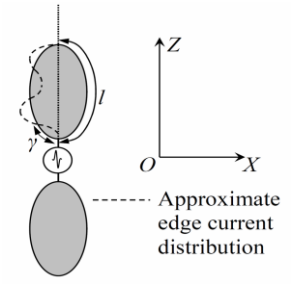

Fig. 4. Patch dipole

As an example, we have synthesized an antenna with a slightly increasing gain between 600 MHz and 1.5 GHz. The minimum gain was set to 2 dBi and the maximum gain to 4 dBi, respectively.

The profile resulting by using the proposed approach is given in Fig. 5. It should be emphasized that the profile function was calculated by assuming a given gain variation on a finite frequency domain support. Consequently, the theoretical length of the profile would be infinite. In order to design an antenna with a feasible size, we truncated the calculated profile to the mostly-radiating region, as the contribution of the ripples becomes negligible above a certain value of x.

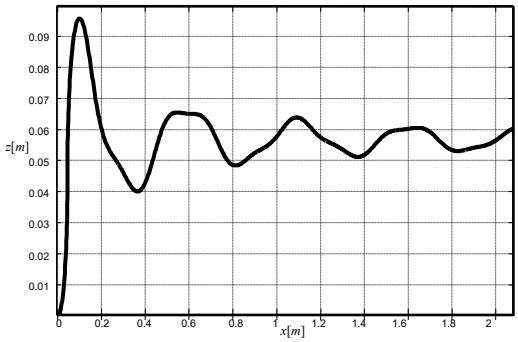

Fig. 5. Profile resulting from synthesis

In order to prove that hypothesis, we considered the corresponding wire profile driven across an infinitesimal gap (the lower arm of the wire dipole can be imagined as a symmetrical profile on the other side of the *OX* axis). We established two regions of analysis on the antenna profile, as it can be seen in Figure 6, and we investigated the contribution to the radiation of each region.

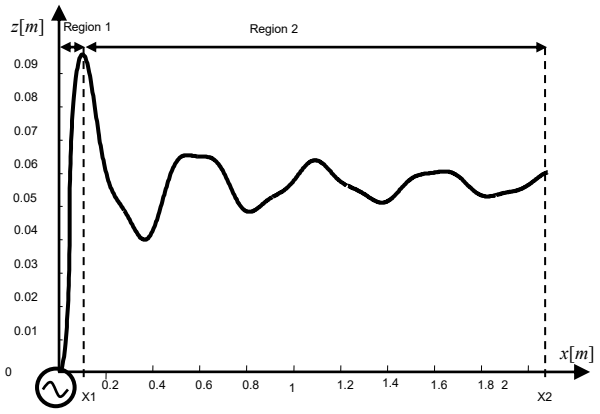

Fig. 6. Hypothetical wire implementation

The ratio between the radiated power densities corresponding to the two regions is shown in Figure 7. It is apparent that Region 2 radiates a power amount at least ten times less then Region 1 between 820 MHz and 1.35 GHz. Thus, the contribution of Region 2 can be neglected almost all over the frequency range. The synthesized profile can therefore be truncated to the first region, as in Figure 8.

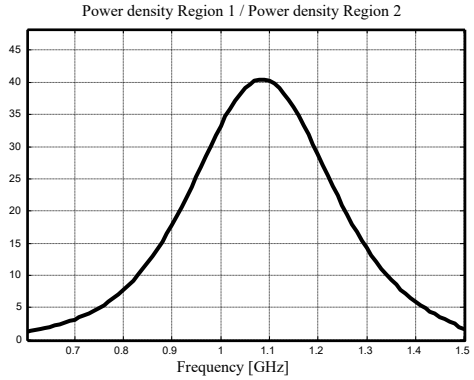

Fig. 7. Ratio between radiated power densities corresponding to the two regions

In that case, the proposed synthesis approach led to a dipole with circularly-shaped arms; the arm diameter is 10 cm. Antennas of this kind type have already been reported as operating over an ultra-wide band [25].

In order to validate the proposed synthesis method, the resulting antenna was simulated. Furthermore, the antenna was also manufactured (Figure 9) and measured. We used a FR4 substrate with a dielectric constant of 4.7, a loss tangent of 0.017, and a thickness of 1.6 mm. The design obviously took into account those substrate parameters.

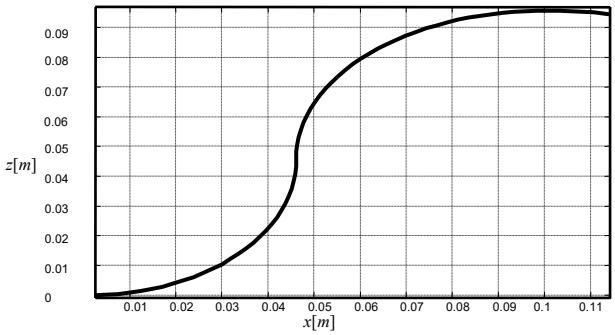

Fig. 8. Synthesized profile truncated to region 1

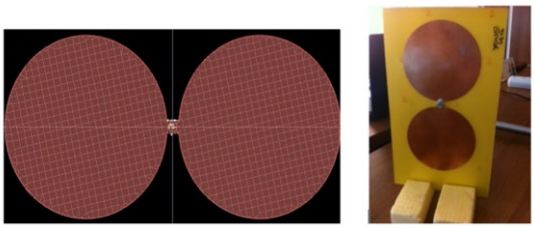

Fig. 9. Resulting design: simulation layout and manufactured antenna

Figure 10 shows the gain variation issued from simulation and measurements. It can be noted that the simulated gain has indeed a quasi-linear increase from 2dBi to 4 dBi, as the frequency ranges from 600 MHz to 1.5 GHz. As expected, the closest gain variation to the linear one is achieved for frequencies between 820 MHz and 1.35 GHz.

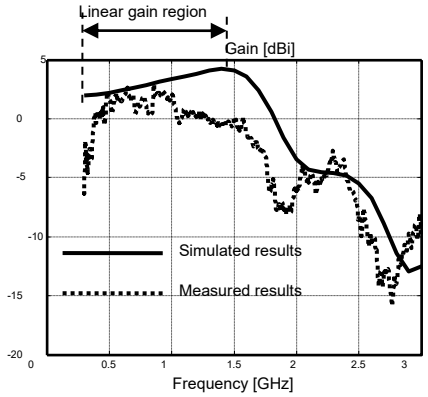

Fig. 10. Antenna gain: measured and simulated results.

Although gain measurements took into account the variation of the input impedance of the antenna, the difference between simulated and measured results is actually due to the common mode currents on the coaxial line [26]. However, the physical antenna still has a quasi-flat response over a wide frequency range, so it was successfully used for spark detection applications.

4. Time-domain response shaping

Let us consider as $v_g(t)$ the first derivative of a Gauss pulse. The bandwidth at –3dB of such a waveform is usually in the order of the central frequency of its spectrum. We aim to design a planar dipole that radiates the same time-domain waveform at a direction perpendicular to its plane.

In that case, a length $l = c_0\ t_{supp}$ for each dipole arm would provide a good radiation efficiency and the time-domain radiation should be investigated within a time slice of $2t_{supp}$. That ensures that the reflected pulse generated at the open end of the antenna has completely passed beyond the source end. The time support was defined at 0.01% of the pulse magnitude.

Figure 11 shows the expansion functions in (12) for N=11 and Figure 12 gives the resulting weights, e_n.

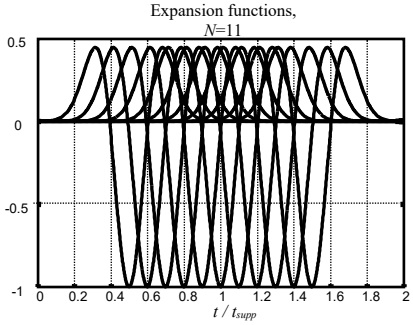

Fig. 11. Expansion functions for an excitation proportional to the first derivative of a Gauss pulse

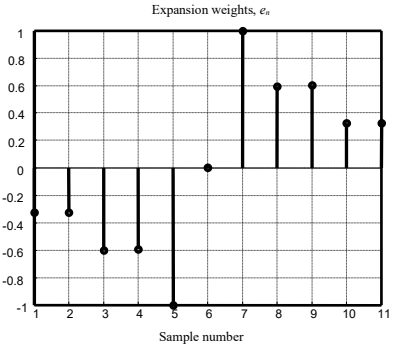

Fig. 12. Field expansion weights for an excitation proportional to the first derivative of a Gauss pulse, N=11

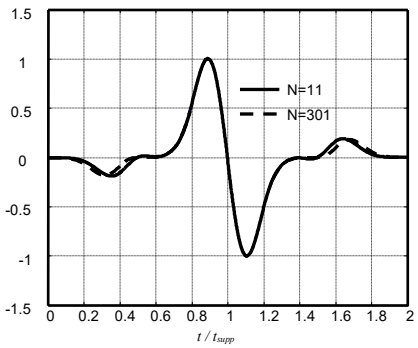

Fig. 13. Antenna response reconstructed with the synthesis weights

It should be noted that the shape of the approximated response reconstructed with the synthesis weights would not improve by increasing the number of terms (Figure 13). The difference between the excitation waveform and the reconstructed one is mainly due to the finite length of the support.

One possible wire profile is shown in Figure 14.

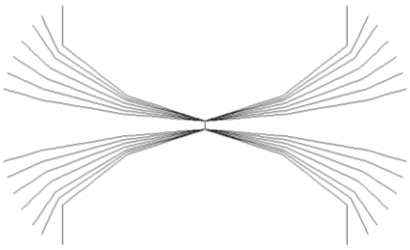

Fig. 14. Wire model of the synthesized antenna. Arm length: $l = c_0\, t_{supp}$

For each arm, the cosines of the angles between the wire segments and the *OZ* axis are in the same ratio as the expansion weights in Figure 12. It should be emphasized that there is no unique current profile complying with a given set of weights. In order to improve the input matching figure, several arms with the same projection ratio can be used.

The impulse response of the wire design was found by using GNEC and an inverse Fourier transform. Figure 15 shows the time-domain waveform of the normalized far-electric field. A good fidelity figure was achieved, although the expansion contains relatively few terms and some effects (e.g., the mutual coupling between segments) were neglected.

The input matching of an antenna with pulsed excitation can be quantified as an energy reflection coefficient [5],

$$g = \sqrt{\frac{\text{Energy of the reflected signal}}{\text{Energy of the incident signal}}} = 2\sqrt{\frac{\mathcal{R}_{v_r,v_r}(0)}{\mathcal{R}_{v_g,v_g}(0)}} \tag{16}$$

in which $v_r(t)$ is the reflected waveform at the antenna input, and $\mathcal{R}_{v_g,v_g}(t)$, $\mathcal{R}_{v_r,v_r}(t)$ stand for the autocorrelation functions of the forward- and reflected-input waveforms.

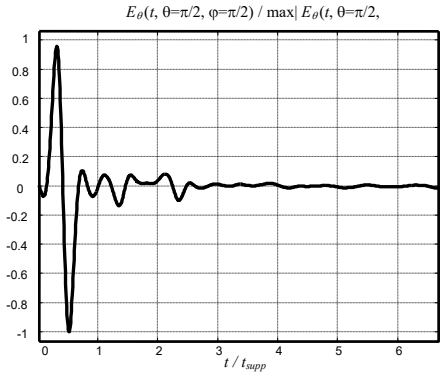

Fig. 15. Time-domain response of the synthesized antenna

An energy-based descriptor similar to the frequency-domain VSWR; i.e., the pulse matching ratio [5] can be defined as

$$s = \frac{1+g}{1-g}. \tag{17}$$

The energy gain [1] is an important figure of merit concerning the radiation of UWB antennas,

$$G(\theta,\varphi) = \frac{4\pi \cdot \text{Energy radiated per unit solid angle}\,(\theta,\varphi)}{\text{Total radiated energy}} = \frac{16\pi Z_0}{\eta_0}\frac{\mathcal{R}_{e_t(\theta,\varphi),e_t(\theta,\varphi)}(0)}{\mathcal{R}_{v_g,v_g}(0)} \tag{18}$$

where η_0 is the free space wave impedance and Z_0 the normalizing impedance at the antenna input. This gain figure is generally defined by using as a reference, the maximum available energy at the source.

The similarity between the radiated waveform, $e_t(t)$ and the activation waveform, $v_g(t)$ is commonly expressed by the fidelity factor [1]

$$\begin{aligned} K_{v_g,e_t(\theta,\varphi)}(\theta,\varphi) &= \frac{\text{Correlated energy}\,(\theta,\varphi)}{\sqrt{\text{Input energy} \cdot \text{Energy radiated per solid angle}\,(\theta,\varphi)}} \\ &= \frac{\mathcal{R}_{v_g,e_t(\theta,\varphi)}(0)}{\sqrt{\mathcal{R}_{v_g,v_g}(0)\cdot\mathcal{R}_{e_t(\theta,\varphi),e_t(\theta,\varphi)}(0)}}. \end{aligned} \tag{19}$$

The antenna design in Fig. 14 exhibits a value of s=5.84 on a normalizing impedance of 50Ω. The fidelity factor is K=0.973 and the energy gain is G= 2.16dB for $v_g(t)$ given above.

Such a planar dipole grants minimal distortion at a single direction; i.e., the perpendicular one. However, many applications require omni-directional coverage at least in one plane. That is, the antenna should be a revolving body. The simplest pulse-matched radiating body can be designed by properly shaping a conducting strip on a cylindrical surface. The decoiled strip can actually be shaped as piecewise straight edge with slope ratios according to the synthesis weights, provided that

$$a/c_0 << t_{supp} \tag{20}$$

where a is the radius of the cylinder. That condition means that there is no significant delay between points lying at the same height on the cylindrical core. In practice, an a/c_0 in the order of t_{supp} / 30 yields good results.

More complicated revolution bodies can be imagined; nevertheless, the effect of the delay between points at the same height on their surface cannot be neglected anymore and should therefore be included in the computation of the synthesis weights.

In order to provide a good input-matching figure, each arm of the antenna that we propose next consists of two equally spaced, positive sloped strips. Each of them

covers a sector of 90° on the cylindrical support (Figure 16). The slopes of the decoiled strips were the same as for the inner arms of the planar design in Figure 14. We took $l=c_0\ t_{supp}$ and $a=c_0\ t_{supp}$ /30. Figure 17 gives the normalized radiation field waveform computed with the simulated impulse response of the antenna.

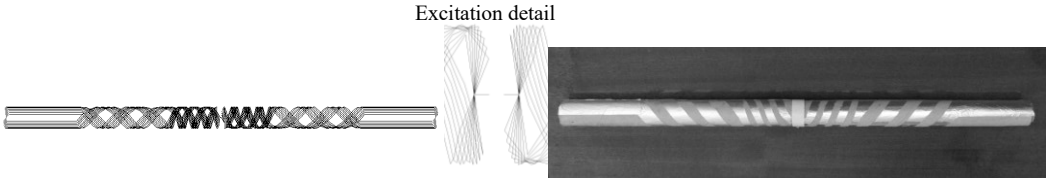

Fig. 16. Cylindrical spiral dipole: antenna model and physical implementation

The values of the relevant descriptors for the above antenna design are s=4.66, $K(\theta=90°)$=0.954, and $G(\theta=90°)$= 0.1dB, respectively. The energy gain is lower than of the planar dipole, but it is in the order of the figures reported for other cylindrical configurations, with the same aspect ratio [20].

As shown before, the fidelity factor does not essentially depend on φ. A good fidelity figure is still obtained for small variations of θ; for example, K=0.93 at θ=70° (Figure 18).

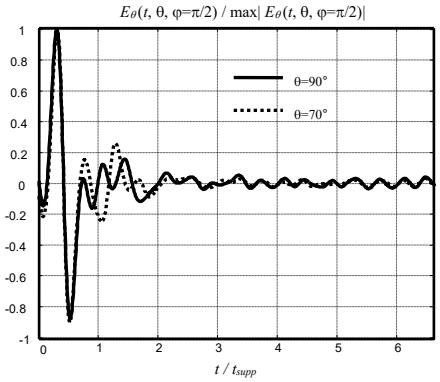

Fig. 17. Time-domain response of the cylindrical spiral dipole: data based on the simulated impulse response

The pulse matching ratio, s is still high. The simulator that we are currently using does not accurately model all practical configurations of excitation. We therefore fabricated and measured such a cylindrical, spiral dipole. The core of the prototype was a carton cylinder with an outer diameter of 28 mm.

The total length of each conducting strip was 420 mm, and they were shaped as explained before. The antenna was designed for military applications with a pulsed excitation centered on 700 MHz. For an activation waveform as before, we found s=3.6.

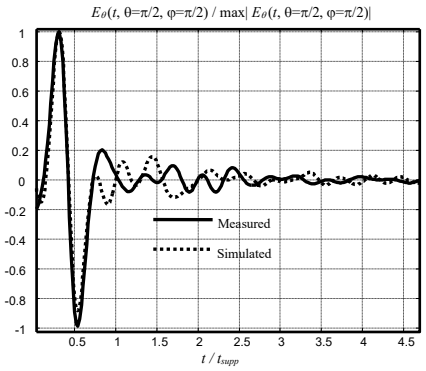

Fig. 18. Time-domain response of the cylindrical spiral dipole: data based on the measured impulse response vs. simulation

Conclusions

A synthesis method based on variable slope profiles was presented. The applicability to the frequency-domain synthesis was demonstrated by designing antennas with a given gain profile over a frequency band. The method was successfully validated for a patch dipole with a slightly increasing gain over a given frequency range. The method can be used also for a linear gain variation. In the time-domain, our synthesis procedure may lead to an optimal design for a precise waveform of excitation. Hence, the resulting antenna might not yield a low-distortion response for activation waveforms, other than that for which the synthesis was performed. Although the energy gain is generally in the order of 0dB, all the antenna configurations provide a good fidelity, along with a good input matching figure.

R E F E R E N C E S

[1] J. S. McLean, H. Foltz and R. Sutton, IEEE Trans. Antennas Propag., **53**, 553 (2005).

[2] J. S. McLean and R. Sutton, *UWB Antenna Characterization* (Proc. of the IEEE International Conference on Ultra-Wideband, Hannover, Germany, 2008).

[3] T. Dissanayake and K. P, Esselle, IEEE Trans. Antennas Propag., **54**, 3184 (2006).

[4] C. G. Rego, J. S. Nunes and M. N. de Abreu Bueno, *Unified characterization of UWB antennas in time and frequency domains: an approach based on the Singularity Expansion Method* (Proc of the Microwave and Optoelectronics Conference, Salvador, Brazil, 2007).

[5] R. D. Tamas, L. Babour and E. Fond, *Energy-based input reflection coefficient for the characterization of ultra-wide band antennas*, (Proc. of the IEEE International Workshop on Antenna Technology, Chiba, Japan, 2008).

[6] Z. N. Chen, *UWB Antennas with Enhanced Performances*, (Proc. of the International Conference on Microwave and Millimeter Wave Technology, Nanjing, China, 2008).

[7] X. Ze-ming and D. Huan-huan, *A Novel UWB Time-domain Antenna Based on GA* (Proc. of the Asia-Pacific Microwave Conference, 2010).

[8] L. Babour, E. Fond, R. D. Tamas, and P. Saguet, *An UWB folded dipole antenna: Time and frequency domain characterization* (Proc. of the 2nd European Conference on Antenna and Propagation, Edinburgh, UK, 2007).

[9] M. Ciattaglia and G. Marrocco, IEEE Trans. Antennas Propag., **56**, 1928 (2008).

[10] J. L. Quijano and G. Vecchi, IEEE Trans. Antennas Propag., **58**, 727 (2010).

[11] S. Chamaani, M. S. Abrishamian and S. A. Mirtaheri*, IEEE Antennas and Wireless Propagation Letters,* **9**, 666 (2010).

[12] D. C. Chang, C. H. Liao and P. Hsu, *UWB Antenna Array* (Proc. of the IEEE International Workshop on Antenna Technology, Hong Kong, China, 2011).

[13] D. C. Chang and C. H. Liao, *Performances of UWB Antenna and Array* (Proc. of the IEEE-APS Topical Conference on Antennas and Propagation in Wireless Communications, Cape Town, South Africa, 2012).

[14] H. G. Schantz, *Directive, electrically-small UWB antennas* (Proc. of the IEEE International Conference on Ultra-Wideband, Syracuse, NY, USA, 2012).

[15] Z. Raida, J. Lacik and Z. Lukes, *Multi-objective synthesis of multiband planar antennas in time domain*, (Proc. of the International Conference on Electromagnetics in Advanced Applications, Torino, Italy, 2007).

[16] L. Lizzi, G. Oliveri and A. Massa, *Exploitation of spline-based geometries for the time-domain synthesis of UWB antennas* (Proc. of the 5th European Conference on Antennas and Propagation (EUCAP), Rome, Italy, 2011).

[17] L. Lizzi, L. Manica and A. Massa, *Time domain analysis for UWB antenna synthesis*, (Proc. of the European Microwave Conference, Rome, Italy, 2009).

[18] W. Wiesbeck, G. Adamiuk and C. Sturm, Proceedings of the IEEE, **97**, 372 (2009).

[19] S. Zwierzchowski and M. Okoniewski, *Antennas for UWB Communications: A Novel Filtering Perspective*, (Proc. of the IEEE Antennas and Propagation Society International Symposium, Monterey, California, USA, 2004).

[20] R. D. Tamas, L. Babour, E. Fond, J. Chilo and P. Saguet, Microwave Opt. Technol. Lett., **50**, 917 (2008).

[21] C. A. Balanis, *Antenna Theory – Analysis and Design* (Wiley, New York, USA, 1997).

[22] R. D. Tamas, T. Petrescu and G. Caruntu, *On Some Implementation Issues for Time-Domain, Pulse-Matched Synthesized Antennas* (Proc. of the IEEE International Workshop on Antenna Technology, 2012).

[23] R. D. Tamas, D. Deacu, G. Caruntu and T. Petrescu, *An Indoor Measuring Technique for Antenna Gain* (Proc. of the IEEE International Workshop on Antenna Technology, 2013).

[24] L. Babour, E. Fond, R. Tamas, P. Saguet and S. Perrot, *A folded dipole antenna for UWB applications* (Proc. of the UWB 2007 European Workshop, 2007).

[25] A. G. Yarovoy, R. Pugliese, J. H. Zijderveld and L.P. Ligthart, *Antenna Development for UWB Impulse Radio* (Proc. of the 34th European Microwave Conference, 2004).

[26] A. V. Vorobyov, J. H. Zijderfeld, A. G. Yarovoy and L. P. Ligthart, *Impact Common mode currents on miniaturized UWB antenna Performance* (Proc. of the European Conference on Wireless Technology, 2005).